치의학석사 학위논문

Analysis of brain connectivity during nitrous oxide sedation using graph theory

그래프 이론을 이용한 아산화질소 진정 동안의 뇌 연결성 변화에 관한 연구

2018년 2월

서울대학교 대학원

치의과학과 소아치과학 전공

이 지 민

Abstract

Analysis of brain connectivity during nitrous oxide sedation using graph theory

Ji Min Lee

School of Dentistry, Department of Pediatric Dentistry

The Graduate School

Seoul National University

(Directed by Prof. Teo Jeon Shin)

Nitrous oxide, the least potent inhalation anesthetic, is widely used for conscious sedation. Recently, it has been reported that the occurrence of anesthetic-induced loss of consciousness decreases the interconnection between brain regions, resulting in brain network changes. However, few studies have investigated these changes in conscious sedation using nitrous oxide. Therefore, the present study aimed to use graph theory to analyze changes in brain networks during nitrous oxide sedation.

Participants were 20 healthy volunteers (10 men and 10 women, 20–30 years old) with no history of systemic disease. We acquired electroencephalogram (EEG) recordings of 32 channels during baseline, nitrous oxide inhalation sedation, and

recovery. EEG epochs from the baseline and the sedation state (50% nitrous oxide) were extracted and analyzed with the network connection parameters of graph theory.

Analysis of 1/f dynamics, revealed a steeper slope while in the sedation state than during the baseline. Network connectivity parameters showed significant differences between the baseline and sedation state, in delta, alpha1, alpha2, and beta2 frequency bands. The most pronounced differences in functional distance during nitrous oxide sedation were observed in the alpha1 and alpha2 frequency bands.

Change in 1/f dynamics indicates that changes in brain network systems occur during nitrous oxide administration. Changes in network parameters imply that nitrous oxide interferes with the efficiency of information integration in the frequency bands important for cognitive processes and attention tasks. Alteration of brain network during nitrous oxide administration may be associated to the sedative mechanism of nitrous oxide.

Keywords : Graph theory, Nitrous oxide, Sedation, Electroencephalogram (EEG)

Student Number : 2016-22044

Table of Contents

I. Introduction

Behavior management required for children with severe anxiety and fear can lead to difficulties in obtaining high quality dental care. In adults, pain or anxiety may cause reluctance to receiving dental treatment. In particular, in patients with a history of syncope due to severe stress, dentists should attempt to minimize stress, ensure that patients are comfortable with the treatment, and consider the use of sedation during dental treatment.

Nitrous oxide is a sedative, widely used in medicine and dentistry due to its sedative and analgesic effects, fast onset and recovery, and lack of serious side effects. Sedation refers to the intermediate state between consciousness and total loss of consciousness, in which consciousness is suppressed. Nitrous oxide is the least potent inhalation anesthetic, and induces a minimally conscious sedation state allowing patients to respond appropriately to physical stimuli or verbal commands[1].

The brain is a complex network, and recently using the graph theoretical approach, the structural and functional network of the brain has been shown to have similar properties as those of other complex network systems[2]. Graph theory is a mathematical field that attempts to understand and analyze social phenomena, nature, and network structure, by simplifying them to graphs, defined as a set of nodes (also called "vertices") connected by edges (also called “lines”). Despite differences in the details of each system element, the complex network is known to have similar macroscopic behavior[3]. Using graph theory, the meaning of each node or edge of the system becomes irrelevant. Therefore, the same network analysis can be applied[4] and the efficiency of information exchange within a network can be

mathematically explained.

From this point of view, the brain network is a huge complex network system that consists of nodes represented by neurological elements such as neurons or brain regions, and connecting edges, represented by axonal projections or synapses. One characteristic of this complex network is small world topology[3,5], which features efficient local and long distance connections[6]. Another characteristic of brain networks is the 1/f dynamics that arise from normal spontaneous neural activity[7,8]. Previous studies have reported loss of small world topology[9-11], and changes in the patterns of 1/f dynamics[12,13], in patients with neurological disease. Additionally, brain network and functional connectivity are altered by anesthetic-induced loss of consciousness[14,15].

Taken together, this suggests that brain networks may be altered by subtle changes in consciousness level. However, changes in functional connectivity during nitrous oxide sedation are yet to be demonstrated from the global brain network perspective. Therefore, the aim of this study was to use graph theory to analyze brain network changes during nitrous oxide sedation.

II. Materials and Methods

2.1 Volunteer recruitment

All experimental procedures were approved by the Institutional Review Board (IRB No: CRI15022) Seoul National University Hospital, Seoul, Korea). Participants were 20 healthy volunteers between the ages of 20-28 (10 men: 23-28 years old, mean age: 24.9, and 10 women: 20–28 years old, mean age: 23.5), that all provided written informed consent. Physical examinations and interviews were conducted to confirm that participant had no history of cardiovascular, respiratory, renal, endocrine, hematologic, gastrointestinal, central nervous system, or psychiatric disease. Participants who had such medical disease were excluded from this study.

2.2 Nitrous oxide sedation protocol

The nitrous oxide sedation protocol consisted of four stages. Prior to nitrous oxide administration, baseline electroencephalogram (EEG) recordings were made for 5 min. Subsequently, using a facemask suited to the participant, 100% oxygen was administered at a flow rate of 6 L/min, to confirm appropriate breathing. Sequential administration of 30% and 50% nitrous oxide for 5 min each, respectively, was performed. After nitrous oxide administration, 100% oxygen was administered for 5 min until consciousness returned to baseline. Participants were instructed to fast for 8 h before the experiment, and to keep their eyes closed and relaxed during the EEG recordings. During the experiment, we verified the state of consciousness and sedation by responses to verbal commands.

2.3 EEG signal acquisition

Continuous EEG recordings were obtained from all participants (sampling rate = 2048 Hz, low passed with 417-Hz cutoff frequency). EEG data were acquired with custom-made software (Biosemi, https://www.biosemi.com/), and 32 electrodes were placed according to standard 10-20 International placement (Fp1, AF3, F7, F3, FC1, FC5, T7, C3, CP1, CP5, P7, P3, Pz, PO3, O1, Oz, O2, PO4, P4, P8, CP6, CP2, C4, T8, FC6, FC2, F4, F8, AF4, Fp2, Fz, Cz). Data were saved and analyzed offline. Data were down-sampled at 128 Hz with a 60-Hz notch filter. All data were manually inspected by the researchers to exclude artifacts such as electromyogram (EMG) or electrocardiogram (ECG). Average Fourier cross-spectral matrices were computed for frequency bands including, delta (2–3.5 Hz), theta (4–7.5 Hz), alpha1 (8–9.5Hz), alpha2 (10–12.5 Hz), beta1 (13–18 Hz), beta2 (18.5–21 Hz), beta3 (21.5–30 Hz), and gamma (30.5–44 Hz).

2.4 1/f dynamics

The power spectrum (PS) of EEG, is a biological time series, and often follows a relationship of decreasing power with frequency, and thus, can be expressed as a function of frequency (f) by the following: $PS(f) = \psi * f^{-\alpha}$ [16]. α represents the rate of power spectrum decrease in $\log(PS(f))$ such that $\log(PS(f)) = -\alpha * \log(f) + \log(\psi)$. Therefore, α can provide an estimate of the length (or "distance") of the linear correlations within a given time series[17]. This indicates that α, the slope of the power spectrum, may be able to provide an index of "temporal memory effects" in the time series[17]. This may explain the characteristics of two types of extreme

noise: white and Brownian noise. White noise does not correlate to time and therefore, is not related to frequency bands. The lack of correlation causes the flat power spectrum of white noise. Brownian noise (or random walk noise), displays correlations over time indicating that, in a "random walk" pattern, the position of a particle at time t + 1, depends on its position at time t. Correlations of the time domains can be expressed in relation to frequency domains[17]. The power spectra of white and Brownian noise are proportional to $f^{-\alpha}$, with $\alpha = 0$ and 2, respectively. The power spectrum of spontaneous neural signals may follow the general rule $f^{-\alpha}$, with α close to 1[17]. "Pink noise" or 1/f noise is expressed with $\alpha = 1$, which is in between that of white and Brownian noise.

The exponent α can be obtained by a linear regression analysis of the log(PS) and frequency f, which is expressed as: $\log(PS(f)) = -\alpha * \log(f) + \beta$ ($\beta = \log(\psi)$). We calculated α for each artifact-free epoch, for values ranging from f = 2 to f = 44 Hz. The mean α was calculated for all individual epochs during the baseline and nitrous oxide sedation states. Regression analysis using the "polyfit" function in Matlab (MathWorks, Natick, MA, USA), was used to calculate the slope for each state (baseline or sedated), at all regions of the 32 sensors.

2.5 Lagged phase coherence

Lagged phase coherence between two signals is the amount of crosstalk between the signals from two source activity regions[18]. Because the two sources oscillate coherently with a phase lag, the crosstalk between them can be interpreted as information sharing through axonal transmission. In the discrete Fourier transform, a signal is decomposed to a finite series of sine waves at Fourier frequencies. The

lag in sine waves could be interpreted as a phase shift between two signals. Pascual-Marqui et al.[19] described the threshold of significance for a given lagged phase coherence value based on asymptotic results. Lagged phase coherence was determined for all pairs of sensors. We further analyzed the 32 × 32 functional connectivity matrices for each frequency band in each state. Pearson correlation analysis was used to investigate the relationship between the Functional connectivity value for each pair-wise combination of sensors and physical distance. The physical distance between sensors was calculated using Euclidean distance, calculated using the x, y, and z coordinates of each sensor, obtained using the sLORETA program (http://www.uzh.ch/keyinst/loreta.htm)[20].

2.6 Brain Connectivity Tool Box (BCT) analysis

Node strength, functional distance, characteristic path length, clustering coefficient, local efficiency, and cross-frequency correlations were calculated from the baseline and sedation functional connectivity matrices, based on sensors from the Brain Connectivity Tool Box (BCT) (Version 2017-15-01)[21].

Node strength is defined as the sum of the weight of all connections between the target node and remaining nodes in the network. Functional distance is defined as the length of the shortest path between a pair of nodes. The functional distance matrix was computed from the connection-length matrix using Dijkstra's algorithm[22]. Characteristic path length is defined as the average shortest path length of the network, which is the mean functional distance matrix in which the distance between two nodes is not infinity. The clustering coefficient measures the degree of local connectivity between each node and its neighbors and is calculated

by estimating the number of triangles around a node. Local efficiency is a parameter that characterizes the efficiency of information transfer between the neighbors of a particular node. Local efficiency is obtained by calculating the average inverse shortest path length for the subnetwork formed by node neighborhoods.

2.7 Statistical analysis

A Wilcoxon signed-rank test was used to detect differences between the baseline and sedative state for each network connectivity measurement and slope steepness. A Mann-Whitney U test was used to detect any potential gender differences in network parameters. P values less than 0.05 were considered statistically significant.

III. Results

3.1 1/f dynamics

The slope of the baseline was significantly steeper than that of the sedation state (p<0.001), indicating a shift to a more-random network (Fig. 1).

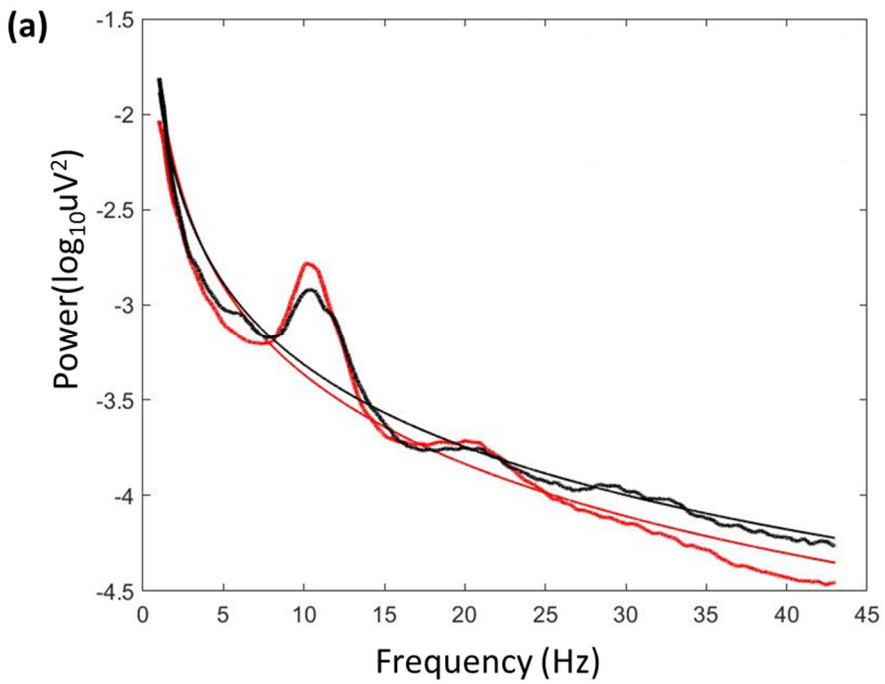

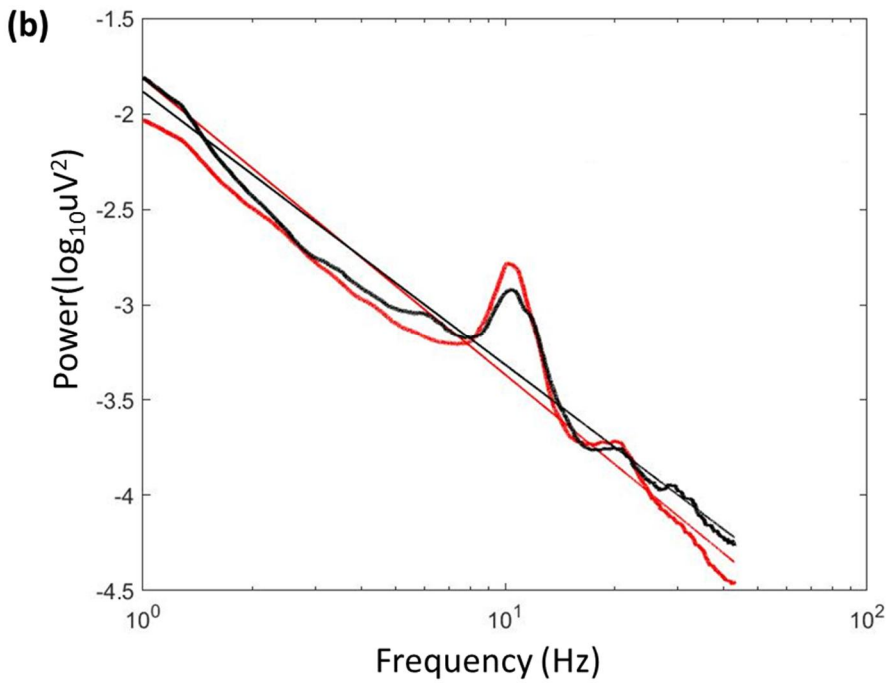

Fig. 1. (a) The representative of 1/f dynamics for the baseline (red) and the sedation state (black). (b) The representative of log-dynamics for the baseline (red) and the sedation state (black).

3.2 Network connectivity analysis

We found an overall difference between the baseline and the sedation state, in the mean values of connectivity strength, node strength, clustering coefficient, local efficiency, and characteristic path length. Specifically, during the sedation state, delta, alpha1, alpha2, and beta2 frequency bands had significantly lower connective strength, node strength, clustering coefficient, and local efficiency, than during the baseline. Characteristic path length was significantly higher in the sedation state compared to the baseline (Fig. 2). No differences in any network parameters were observed between males and females (data not shown). For all

network parameters, the most prominent differences between the baseline and sedation state were seen in the alpha1 and alpha2 frequency bands.

Differences in brain network connectivity between the baseline and sedation state are summarized in Table 1.

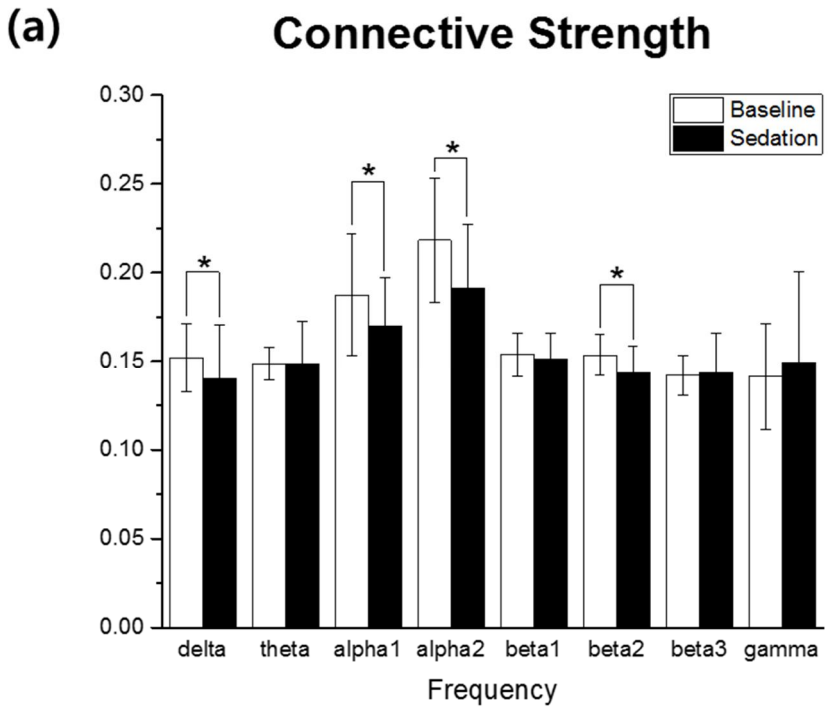

(b)

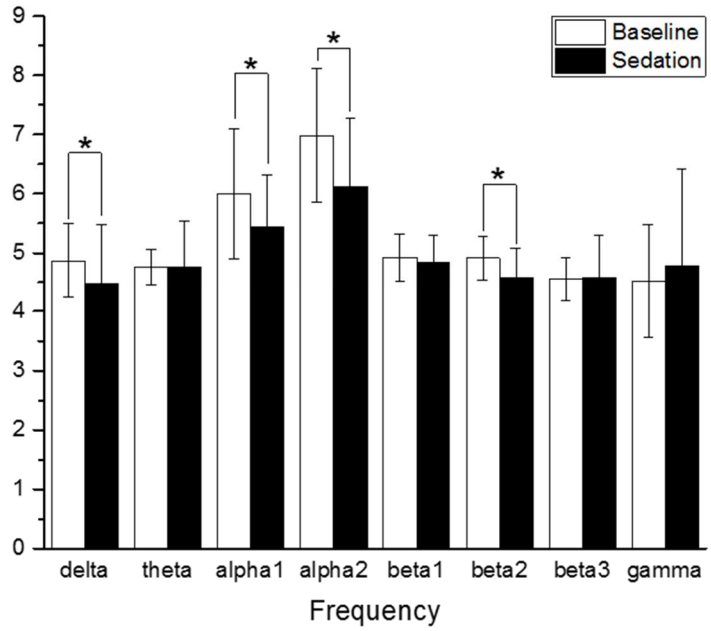
Node Strength
Baseline
Sedation
9
8
7
6
5
4
3
2
1
0
*
*
*
*
delta
theta
alpha1
alpha2
beta1
beta2
beta3
gamma
Frequency

(c)

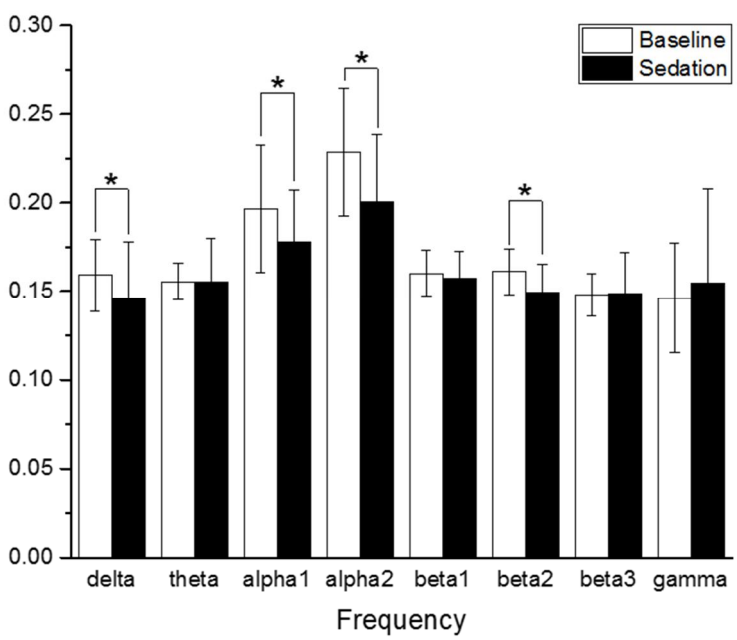
Local Efficiency
Baseline
Sedation
0.30
0.25
0.20
0.15
0.10
0.05
0.00
*
*
*
*
delta
theta
alpha1
alpha2
beta1
beta2
beta3
gamma
Frequency

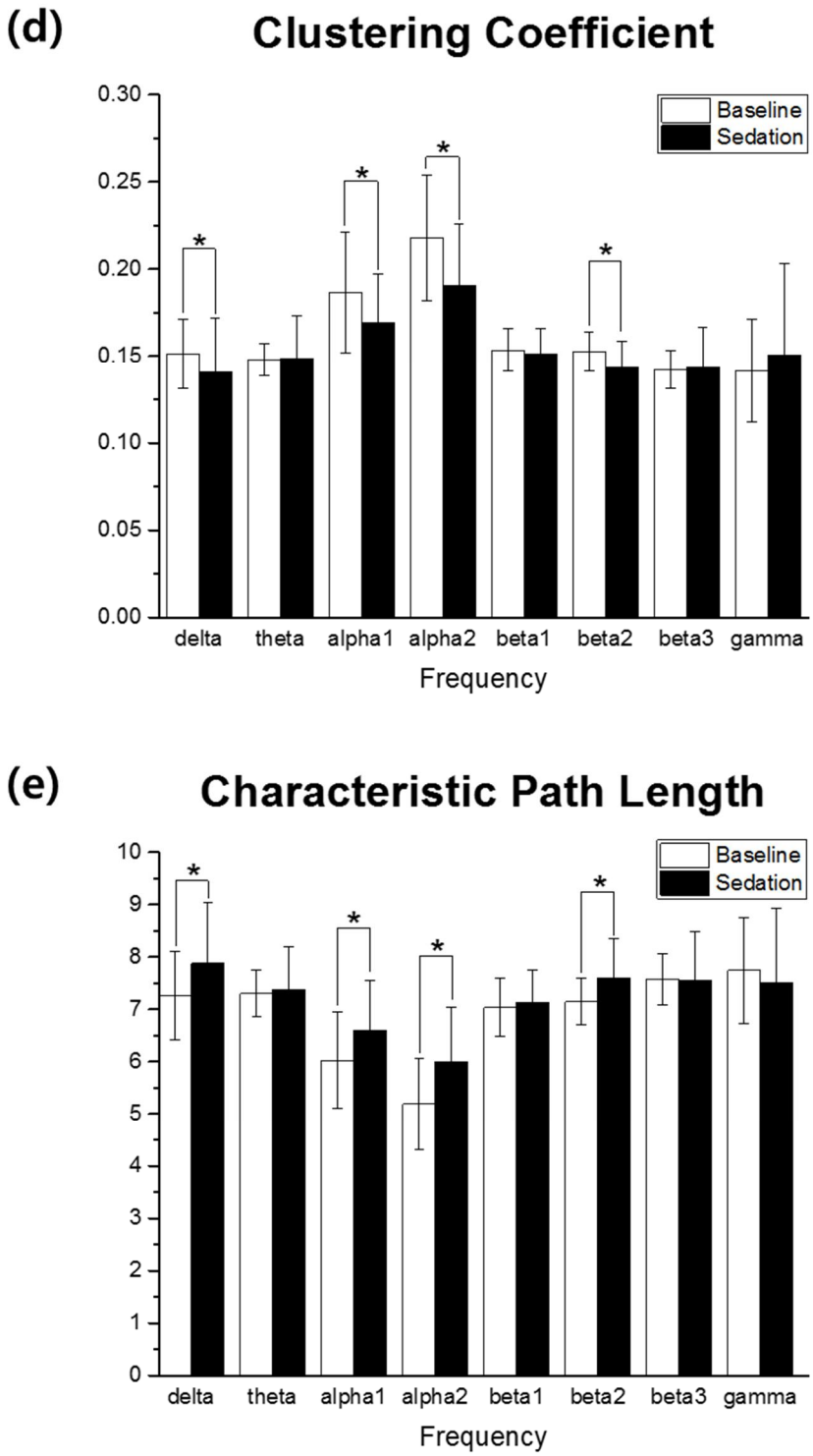

Fig. 2. Network connectivity parameters of the baseline (red) and the sedation state (black) frequency bands. (a) Connectivity strength, (b) Node strength, (c) Local

efficiency, (d) Clustering coefficient, and (e) Characteristic path length (*p<0.05).

Table 1. Mean value and standard deviation of network connectivity parameters between the control and sedation state (*p<0.05).

Parameter	Frequency	state	Mean	SD	p Value
Connective strength	delta	Baseline	0.152	0.020	0.006*
	delta	Sedation	0.140	0.031	
	theta	Baseline	0.149	0.010	0.100
	theta	Sedation	0.149	0.024	
	alpha1	Baseline	0.187	0.034	0.037*
	alpha1	Sedation	0.170	0.028	
	alpha2	Baseline	0.218	0.035	0.003*
	alpha2	Sedation	0.191	0.036	
	beta1	Baseline	0.154	0.012	0.478
	beta1	Sedation	0.151	0.014	
	beta2	Baseline	0.154	0.012	0.044*
	beta2	Sedation	0.143	0.015	
	beta3	Baseline	0.142	0.011	0.279
	beta3	Sedation	0.143	0.023	
	gamma	Baseline	0.141	0.030	1.000
	gamma	Sedation	0.150	0.051	
Node strength	delta	Baseline	4.863	0.626	0.006*
	delta	Sedation	4.489	0.982	
	theta	Baseline	4.758	0.306	0.100
	theta	Sedation	4.755	0.775	
	alpha1	Baseline	6.000	1.103	0.037*
	alpha1	Sedation	5.438	0.885	

	alpha2	Baseline	6.986	1.125	0.003*
	alpha2	Sedation	6.121	1.149	
	beta1	Baseline	4.921	0.394	0.478
	beta1	Sedation	4.847	0.457	
	beta2	Baseline	4.916	0.372	0.044*
	beta2	Sedation	4.585	0.492	
	beta3	Baseline	4.552	0.364	0.279
	beta3	Sedation	4.579	0.728	
	gamma	Baseline	4.517	0.962	1.000
	gamma	Sedation	4.787	1.638	
Local efficiency	delta	Baseline	0.159	0.020	0.006*
	delta	Sedation	0.146	0.032	
	theta	Baseline	0.155	0.010	0.100
	theta	Sedation	0.155	0.025	
	alpha1	Baseline	0.197	0.036	0.028*
	alpha1	Sedation	0.178	0.029	
	alpha2	Baseline	0.229	0.036	0.003*
	alpha2	Sedation	0.201	0.038	
	beta1	Baseline	0.160	0.013	0.455
	beta1	Sedation	0.158	0.015	
	beta2	Baseline	0.161	0.013	0.028*
	beta2	Sedation	0.149	0.016	
	beta3	Baseline	0.148	0.012	0.263
	beta3	Sedation	0.149	0.023	
	gamma	Baseline	0.146	0.031	0.970
	gamma	Sedation	0.155	0.053	
Clustering coefficient	delta	Baseline	0.151	0.020	0.006*
	delta	Sedation	0.141	0.031	

	theta	Baseline	0.148	0.009	0.093
	theta	Sedation	0.149	0.025	
	alpha1	Baseline	0.187	0.035	0.040*
	alpha1	Sedation	0.169	0.028	
	alpha2	Baseline	0.218	0.036	0.002*
	alpha2	Sedation	0.190	0.036	
	beta1	Baseline	0.154	0.012	0.478
	beta1	Sedation	0.152	0.014	
	beta2	Baseline	0.153	0.011	0.044*
	beta2	Sedation	0.143	0.015	
	beta3	Baseline	0.142	0.011	0.313
	beta3	Sedation	0.144	0.023	
	gamma	Baseline	0.141	0.030	0.970
Characteristic path length	delta	Baseline	7.268	0.843	0.006*
	delta	Sedation	7.882	1.152	
	theta	Baseline	7.306	0.450	0.086
	theta	Sedation	7.381	0.807	
	alpha1	Baseline	6.033	0.910	0.023*
	alpha1	Sedation	6.602	0.955	
	alpha2	Baseline	5.189	0.869	0.001*
	alpha2	Sedation	5.998	1.050	
	beta1	Baseline	7.040	0.556	0.654
	beta1	Sedation	7.133	0.625	
	beta2	Baseline	7.146	0.444	0.044*
	beta2	Sedation	7.607	0.741	
	beta3	Baseline	7.575	0.493	0.332
	beta3	Sedation	7.562	0.928	
	gamma	Baseline	7.746	1.005	0.823

gamma	Sedation	7.504	1.430

3.3 Functional distance correlation matrices

Differences in Pearson correlations of functional distances between sedation state and baseline were observed for all frequency bands (data not shown). However, the most prominent correlations were observed for the alpha1 and alpha2 frequency bands (Fig. 3). Additionally, the functional distance (in regard to physical distance), was significantly longer in the sedation state than the baseline for the alpha1 and alpha2 frequency bands.

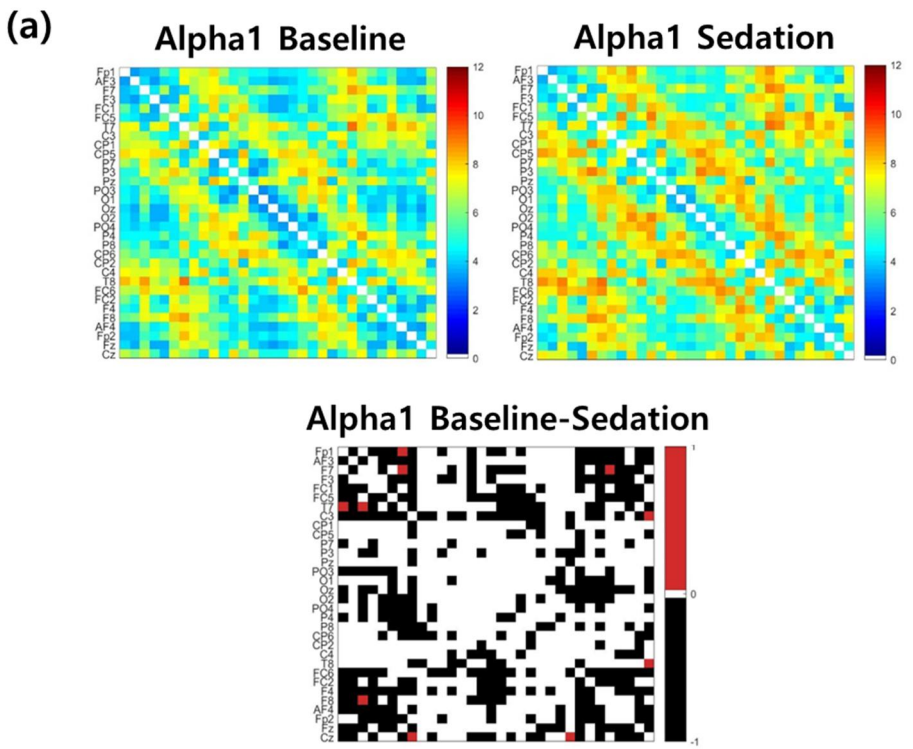

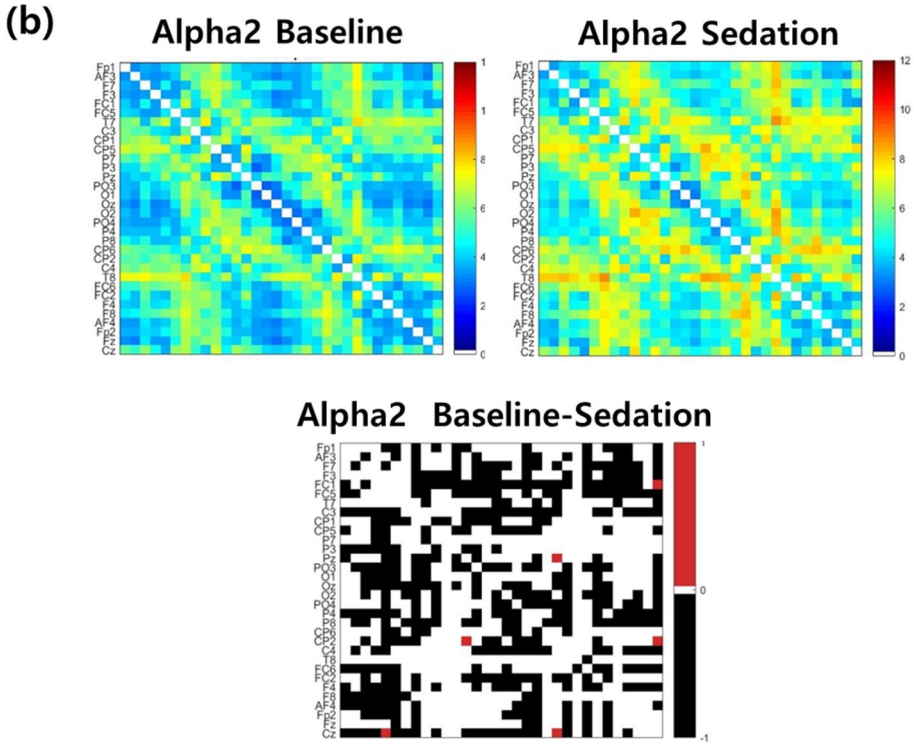

Fig. 3. Correlation matrices of the functional distances for (a) alpha1, and (b) alpha2. In the bottom matrix, red areas indicate a longer functional distance in the baseline. Black areas indicate a longer functional distance in the sedation state. White areas indicate no difference in functional distance.

IV. Discussion

In this study, we used graph theory to analyze EEG data recorded during nitrous oxide sedation. We confirmed that in the sedation state, brain network properties differ from those in the baseline. To the best our knowledge, this is the first study to use graph theory to investigate brain network changes associated with nitrous oxide sedation.

Compared to the baseline, changes in the pattern of 1/f dynamics were observed during the sedation state. Because 1/f dynamics are indicative of overall brain network characteristics, it appears that the brain network changed following nitrous oxide administration. These changes in brain network characteristics have been observed in many neurological diseases, such as schizophrenia[12], autism[13], and anxiety[23]. Consistent with previous studies, brain network dynamics may significantly change during nitrous oxide administration, even though consciousness is only minimally depressed.

Parameters such as connective strength, node strength, clustering coefficient, local efficiency, and characteristic path length, are commonly used as indicators of network connectivity[3,5]. In this study, while in the sedation state, network parameters including the clustering coefficient and local efficiency were decreased, and the characteristic path length was increased, in several frequency bands, suggesting a change in small world network topology. While in the sedation state, a reduction in the efficiency of information processing and distribution is observed, indicated by increased path length resulting from decreased local efficiency. Information integration theory suggests that certain cortical areas can distinguish

and recognize varied information, and information is integrated by the connections between different areas and within these areas[24,25]. Studies using graph theory to analyze the loss of consciousness induced by propofol[26-28], isoflurane[29], and dexmedetomidne[15], have revealed changes in network parameters, suggesting that anesthetics alter the brain functions associated with information transferring processes within the brain network. Consistent with previous research, nitrous oxide interferes with the efficiency of information integration, leading to the transition from the baseline to sedative state.

In addition, changes in connective and node strengths indicate that nitrous oxide changes the quality of information processing in the brain network, and decreases the connection strength between nodes while in the sedation state[24,28]. Contradictory to a previous study in which propofol was reported to increase the clustering coefficient during general anesthesia[26,28], we observed a decrease in the clustering coefficient of sedation. This may be due to differences in the drug used (propofol vs nitrous oxide), and sedation depth. Specifically, changes in brain network properties during nitrous oxide sedation may be caused by different mechanisms than that of the unconscious state induced by propofol.

Brain processes can be accomplished through various frequency interactions[30,31]. The delta band is associated with salience detection and basic biological motivations[32]. In this study, we found a decrease in network parameters in the delta band. Changes in brain activity associated with changes in delta spectral power have been reported to occur when nitrous oxide is used during sevoflurane[33] or isoflurane[34] administration. Additionally, changes in delta band brain activity occur when nitrous oxide is used alone[35,36]. Beta oscillation is involved with various tasks that require the sensorimotor system[30]. We have previously reported that

during nitrous oxide sedation, beta band parietal-frontal interactions are decreased[37]. Similar to previous studies, we observed significant alterations in delta and beta frequency bands during nitrous oxide administration. Considering the association of these frequency bands with cognitive function, changes in the brain network dynamics of these bands may impair consciousness.

In the present study, the effect of nitrous oxide was most prominent in the alpha frequency band compared to the other frequency bands we examined. This supports our previous observation that nitrous oxide exhibits the most pronounced frontal-parietal interactions in the alpha band[37]. Alpha oscillations are suggested to have a prominent role in the functions and communications of the entire brain and body[31]. Alpha band is related to the access of information representing environmental knowledge[38]. The changes in brain connectivity induced by nitrous oxide suggests that sedation occurs due to the influence of alpha bands, and nitrous oxide has previously been shown to affect alpha frequency-associated brain activity[33,37]. Additionally, the alteration of brain activities related to the alpha band, have been found to be associated with the actions of various anesthetics[29,39,40]. Taken together, these findings suggest that the alpha frequency band may serve as a putative mechanism or marker for sedation and anesthesia[29].

Changes of network connective parameters in theta and beta bands were not significant in this study. Theta oscillations are most commonly related to memory processes[41]. Nitrous oxide has been reported to produce impairment of memory function[42]. However, memory alteration was not observed in this study. This may be because the sedation time is not long enough to cause memory alteration. Gamma oscillations are associated with attentive processing of information[43]. However, there were no significant changes in the gamma band when

consciousness is altered. This is because this frequency band may be affected by elimination of artifacts such as EMG and ECG.

However, the present study has several limitations. Even though the same nitrous oxide concentration was administered to all participants, individual differences in the response to this concentration may have affected sedation depth. Although all participants maintained consciousness and responded to verbal commands during nitrous oxide sedation, some changes in mood were observed. Therefore, all participants were in a state of conscious sedation during nitrous oxide administration.

V. Conclusion

In conclusion, nitrous oxide induces changes in the brain network, decreasing the efficiency of information processing in the frequency bands important for cognitive processes. Therefore, the decrease in cognitive processes resulting from brain network changes, may be associated to the sedative mechanism of nitrous oxide.

References

1 Malamed, S. F. *Sedation-E-Book: A Guide to Patient Management*. (Elsevier Health Sciences, 2017).

2 Mears, D. & Pollard, H. B. Network science and the human brain: using graph theory to understand the brain and one of its hubs, the amygdala, in health and disease. *Journal of Neuroscience Research* **94**, 590-605 (2016).

3 Bullmore, E. & Sporns, O. Complex brain networks: graph theoretical analysis of structural and functional systems. *Nature Reviews Neuroscience* **10**, 186-198 (2009).

4 Fornito, A., Zalesky, A. & Breakspear, M. Graph analysis of the human connectome: Promise, progress, and pitfalls. *NeuroImage* **80**, 426-444 (2013).

5 Stam, C. J. & Reijneveld, J. C. Graph theoretical analysis of complex networks in the brain. *Nonlinear Biomedical Physics* **1**, 3-3 (2007).

6 Watts, D. J. & Strogatz, S. H. Collective dynamics of 'small-world'networks. *Nature* **393**, 440-442 (1998).

7 Buzsáki, G. & Mizuseki, K. The log-dynamic brain: how skewed distributions affect network operations. *Nature Reviews Neuroscience* **15**, 264-278 (2014).

8 Allegrini, P. *et al.* Spontaneous brain activity as a source of ideal 1/f noise. *Physical Review E* **80**, 061914 (2009).

9 Sanz-Arigita, E. J. *et al.* Loss of 'small-world'networks in Alzheimer's disease: graph analysis of FMRI resting-state functional connectivity. *PloS*

One **5**, e13788 (2010).

10 Pandit, A. S. *et al.* Traumatic brain injury impairs small-world topology. *Neurology* **80**, 1826-1833 (2013).

11 Ponten, S., Bartolomei, F. & Stam, C. Small-world networks and epilepsy: graph theoretical analysis of intracerebrally recorded mesial temporal lobe seizures. *Clinical Neurophysiology* **118**, 918-927 (2007).

12 Radulescu, A. R., Rubin, D., Strey, H. H. & Mujica-Parodi, L. R. Power spectrum scale invariance identifies prefrontal dysregulation in paranoid schizophrenia. *Human Brain Mapping* **33**, 1582-1593 (2012).

13 Lai, M.C. *et al.* A shift to randomness of brain oscillations in people with autism. *Biological Psychiatry* **68**, 1092-1099 (2010).

14 Lee, U., Müller, M., Noh, G. J., Choi, B. & Mashour, G. A. Dissociable Network Properties of Anesthetic State Transitions. *Anesthesiology* **114**, 872-881 (2011).

15 Hashmi, J. A. *et al.* Dexmedetomidine Disrupts the Local and Global Efficiencies of Large-scale Brain Networks. *Anesthesiology* **126**, 419-430 (2017).

16 Norena, A., Moffat, G., Blanc, J., Pezard, L. & Cazals, Y. Neural changes in the auditory cortex of awake guinea pigs after two tinnitus inducers: salicylate and acoustic trauma. *Neuroscience* **166**, 1194-1209 (2010).

17 Buzsaki, G. *Rhythms of the Brain*. (Oxford University Press, 2006).

18 Congedo, M., John, R. E., De Ridder, D., Prichep, L. & Isenhart, R. On the "dependence" of "independent" group EEG sources; an EEG study on two large databases. *Brain Topography* **23**, 134-138 (2010).

19 Pascual-Marqui, R. D. *et al.* Assessing interactions in the brain with exact

low-resolution electromagnetic tomography. *Philosophical Transactions: Mathematical, Physical and Engineering Sciences* **369**, 3768-3784 (2011).

20 Pascual-Marqui, R. D. Standardized low-resolution brain electromagnetic tomography (sLORETA): technical details. *Methods and Findings in Experimental and Clinical Pharmacology* **24**, 5-12 (2002).

21 Rubinov, M. & Sporns, O. Complex network measures of brain connectivity: uses and interpretations. *NeuroImage* **52**, 1059-1069 (2010).

22 Dijkstra, E. W. A note on two problems in connexion with graphs. *Numerische Mathematik* **1**, 269-271 (1959).

23 Tolkunov, D., Rubin, D. & Mujica-Parodi, L. R. Power spectrum scale invariance quantifies limbic dysregulation in trait anxious adults using fMRI: adapting methods optimized for characterizing autonomic dysregulation to neural dynamic time series. *NeuroImage* **50**, 72-80 (2010).

24 Tononi, G. An information integration theory of consciousness. *BMC Neuroscience* **5**, 42 (2004).

25 Marchant, N. *et al.* How electroencephalography serves the anesthesiologist. *Clinical EEG and Neuroscience* **45**, 22-32 (2014).

26 Lee, H., Mashour, G. A., Noh, G. J., Kim, S. & Lee, U. Reconfiguration of Network Hub Structure after Propofol-induced Unconsciousness. *Anesthesiology* **119**, 1347-1359 (2013).

27 Schröter, M. S. *et al.* Spatiotemporal reconfiguration of large-scale brain functional networks during propofol-induced loss of consciousness. *Journal of Neuroscience* **32**, 12832-12840 (2012).

28 Monti, M. M. *et al.* Dynamic change of global and local information processing in propofol-induced loss and recovery of consciousness. *PLoS*

Computational Biology **9**, e1003271 (2013).

29 Blain-Moraes, S. *et al.* Network Efficiency and Posterior Alpha Patterns Are Markers of Recovery from General Anesthesia: A High-Density Electroencephalography Study in Healthy Volunteers. *Frontiers in Human Neuroscience* **11**, 328 (2017).

30 Herrmann, C. S., Strüber, D., Helfrich, R. F. & Engel, A. K. EEG oscillations: from correlation to causality. *International Journal of Psychophysiology* **103**, 12-21 (2016).

31 Başar, E. & Güntekin, B. A short review of alpha activity in cognitive processes and in cognitive impairment. *International Journal of Psychophysiology* **86**, 25-38 (2012).

32 Knyazev, G. G. EEG delta oscillations as a correlate of basic homeostatic and motivational processes. *Neuroscience & Biobehavioral Reviews* **36**, 677-695 (2012).

33 Pavone, K. J. *et al.* Nitrous oxide-induced slow and delta oscillations. *Clinical Neurophysiology* **127**, 556-564 (2016).

34 Hagihira, S., Takashina, M., Mori, T. & Mashimo, T. The impact of nitrous oxide on electroencephalographic bicoherence during isoflurane anesthesia. *Anesthesia & Analgesia* **115**, 572-577 (2012).

35 Foster, B. L. & Liley, D. T. J. Effects of nitrous oxide sedation on resting electroencephalogram topography. *Clinical Neurophysiology* **124**, 417-423 (2013).

36 Foster, B. L. & Liley, D. T. J. Nitrous Oxide Paradoxically Modulates Slow Electroencephalogram Oscillations: Implications for Anesthesia Monitoring. *Anesthesia & Analgesia* **113**, 758-765 (2011).

37 Ryu, J. H., Kim, P. J., Kim, H. G., Koo, Y. S. & Shin, T. J. Investigating the effects of nitrous oxide sedation on frontal-parietal interactions. *Neuroscience Letters* **651**, 9-15 (2017).

38 Klimesch, W. Alpha-band oscillations, attention, and controlled access to stored information. *Trends in Cognitive Sciences* **16**, 606-617 (2012).

39 Purdon, P. L. *et al.* Electroencephalogram signatures of loss and recovery of consciousness from propofol. *Proceedings of the National Academy of Sciences* **110**, E1142-E1151 (2013).

40 Akeju, O. *et al.* Effects of sevoflurane and propofol on frontal electroencephalogram power and coherence. *The Journal of the American Society of Anesthesiologists* **121**, 990-998 (2014).

41 Colgin, L. L. Mechanisms and Functions of Theta Rhythms. *Annual Review of Neuroscience* **36**, 295-312 (2013).

42 Block, R. I., Ghoneim, M. M., Hinrichs, J. V., Kumar, V. & Pathak, D. Effects of a subanaesthetic concentration of nitrous oxide on memory and subjective experience: Influence of assessment procedures and types of stimuli. *Human Psychopharmacology: Clinical and Experimental* **3**, 257-265 (1988).

43 Fries, P., Reynolds, J. H., Rorie, A. E. & Desimone, R. Modulation of Oscillatory Neuronal Synchronization by Selective Visual Attention. *Science* **291**, 1560-1563 (2001).

국문초록

그래프 이론을 이용한 아산화질소 진정 동안의 뇌 연결성 변화에 관한 연구

이 지 민

서울대학교 대학원

치의학과 소아치과학 전공

(지도교수: 신 터 전)

가장 약한 흡입마취제인 아산화질소는 의식하 진정 시 널리 사용된다. 최근 약물에 의해 의식이 소실될 때 뇌의 영역 간 상호연결이 감소하며 뇌 연결망의 형태가 변화하는 것으로 보고되고 있다. 하지만 현재까지는 아산화질소를 이용한 의식하 진정 시에 이러한 변화에 대한 연구는 거의 이루어지지 않았다. 따라서 본 연구에서는 아산화질소 진정 시 나타나는 뇌 연결망의 변화를 그래프 이론을 이용하여 분석하고자 하였다.

전신 질환의 기왕력이 없는 건강한 20명(남 10, 여 10, 20-30세)의 자원자를 대상으로 연구를 진행하였다. 아산화질소 진정 전, 중, 후의 뇌파의 기록을 위해서 32채널 전극을 가진 장비를 이용하였다. 진정 전과 50% 아산화질소 진정 시의 뇌파의 epoch을 추출하여 두 상태에서의 뇌파 변화를 그래프 이론의 네트워크 연결 지표를 이용하여 분석하였다.

1/f dynamics의 분석 결과, 기울기의 크기는 깨어 있는 상태일 때 보다 진정 상태일 때 더 작은 것으로 나타났다. 네트워크 연결 지표는 깨어있을 때와 진정 상태를 비교하였을 때 delta, alpha1, alpha2, beta2에서 유의한 차이가 나타났다. 아산화질소 진정 동안 functional distances의 차이는 alpha1, alpha2 주파수 대역에서 가장 두드러졌다.

아산화질소 진정 시의 1/f dynamics의 변화는 진정 시 뇌 연결망의 변화가 일어난다는 것을 의미한다. 또한 네트워크 연결 지표 변화는 아산화질소가 인지 과정이나 주의업무와 관련 있는 주파수의 정보 통합 효율성을 저하시키는 것을 나타낸다. 결론적으로 아산화질소 진정 시 나타나는 뇌 연결망 변화는 아산화질소의 진정 메커니즘과 관련이 있음을 시사한다.

주요어 : 그래프 이론, 아산화질소, 진정, 뇌파

학 번 : 2016-22044